Cu(II) immobilization onto a one-step synthesized poly(4-vinylpyridine--*co*-ethylene glycol dimethacrylate) resin: Kinetics and XPS analysis

Danijela D. Maksin[1], Aleksandra B. Nastasović[2], Tatjana N. Maksin[1], Zvjezdana P. Sandić[1,3], Katja Loos[4], Bojana M. Ekmeščić[2], Antonije E. Onjia[1]

[1]*University of Belgrade, Vinča Institute of Nuclear Sciences, Belgrade, Serbia*
[2]*University of Belgrade, ICTM – Center for Chemistry, Belgrade, Serbia*
[3]*University of Banja Luka, Faculty of Science, Banja Luka, B&H (Republic of Srpska)*
[4]*Department of Polymer Chemistry, Zernike Institute for Advances Materials, University of Groningen, Groningen, The Netherlands*

Abstract

Synthesis of an unconventional resin based on 4-vinylpyridine (4-VP) and its Cu(II) sorption behavior were studied. Three samples of macroporous crosslinked poly(4-vinylpyridine-*co*--ethylene glycol dimethacrylate) (P4VPE) with different porosity parameters were prepared by suspension copolymerization by varying the *n*-heptane amount in the inert component. The samples were characterized by mercury porosimetry, elemental analysis and X-ray photoelectron spectroscopy (XPS). The sorption of P4VPE for Cu(II) ions, determined under non-competitive conditions, was relatively rapid, *i.e.*, the maximum capacity was reached within 30 min. The maximum experimental sorption capacity for the sample with the highest values of pore diameter and specific pore volume (sample 3, Q_{eq} = 89 mg g^{-1}) was 17.5 times higher than for the sample with the lowest values of pore diameter and specific pore volume (sample 1, Q_{eq} = 5.1 mg g^{-1}). Since the values for pyridine content in all P4VPE samples were almost the same, it was concluded that the porosity parameters have predominant influence on Cu(II) sorption rates on P4VPE. The sorption behavior and the rate-controlling mechanisms were analyzed using six kinetic models (pseudo-first order, pseudo-second order, Elovich, intraparticle diffusion, Bangham and Boyd models). XPS study clarified the nature of the formed P4VPE-Cu(II) species.

Keywords: 4-vinylpyridine, macroporous copolymer, sorption kinetics, XPS.

Available online at the Journal website: http://www.ache.org.rs/HI/

SCIENTIFIC PAPER

UDC 544.2:678.7/.8:543.5

Hem. Ind. **70** (1) 9–19 (2016)

doi: 10.2298/HEMIND141203007M

The presence of the weakly basic nitrogen in the ring, combined with good acid and oxidation resistance, as well as their thermostability, render vinylpyridine polymers convenient for flocculation and metal sorption [1]. High internal volume accessible to the constituents of the treated solution that are being removed is a prerequisite for any sorbent material. Surface area, pore size distribution and nature of the pores have a critical influence on the type of sorption process. The existence of active functional groups on the sorbent surface facilitates chemical interactions that typically result in effects that are different from and less reversible than physisorption [2]. Poly(vinylpyridine) copolymers are primarily used in sorption applications after treatment with appropriate reagents to introduce a desired functional moiety in order to target specific sorbate species. For example, quaternized poly(4-vinylpyridine-*co*-divinylbenzene), P4VPD, (Reillex™ HPQ) was used for the recovery of metallic species (including radioactive metals) like for Hg(II) sorption [3], Cr(VI) removal from aqueous solutions [4], perrhenate sorption from acid solutions [5], uranium sorption from acidic sulfate solutions [6], pertechnetate sorption from nitric acid solutions [7] and separation of plutonium using nitrate anion exchanger [8]. However, additional functionalization of macroporous copolymers is not always recommended. The problems that potentially arise are undesired side reactions leading to ineffective byproducts, unintentional alterations of pore structure as the consequence of chemical modification, low degree of conversion, etc. Structural rigidity and hydrophobicity of P4VPD are undesirable with respect to complexation of metal ions from aqueous solutions [9,10]. These drawbacks could be overcome by using copolymers synthesized with hydrophilic crosslinker, such as ethylene glycol dimethacrylate (EGDMA) or others, like trimethylolpropane trimethacrylate (TRIM) and *N*,*N*-methylenebisacrylamide (MBA). The study of the sorption abilities of 2-vinylpyridine (2-VP), 4-vinylpyridine (4-VP), or 4-methyl-4'-vinyl-2,2'--bipyridine copolymers synthesized with different dimethacrylate crosslinkers was performed with respect to Cd(II), Co(II), Cu(II), Hg(II) and Ni(II) [10], as well

Correspondence: D.D. Maksin, University of Belgrade, Vinča Institute of Nuclear Sciences, P.O. Box 522, 11000 Belgrade, Serbia.
E-mail: dmaksin@vinca.rs, dmaksin@gmail.com
Paper received: 3 December, 2014
Paper accepted: 23 January, 2015

as on poly(4-vinylpyridine) copolymers crosslinked with oligo(ethylene glycol dimethacrylates) (ethylene glycol dimethacrylate (1EG), triethylene glycol dimethacrylate (3EG) and tetraethylene glycol dimethacrylate (4EG)) used for Co(II), Ni(II), Cu(II) and Hg(II) sorption [9].

To the best of our knowledge, only few papers deal with the application of porous 4VP-based copolymers not further modified to introduce functionalities other than pyridine nitrogen. Porous copolymers of 2-VP and 4-VP crosslinked with divinyl benzene (DVB) were used for Cu(II), Ni(II) and Co(II) sorption [11]. Castro *el al*. used P4VPD as supported Cu(II) polymer catalysts for the catalytic oxidation of phenol at 303 K and atmospheric pressure using air and H_2O_2 as oxidants [12].

In this study, three samples of macroporous crosslinked copolymers of 4-vinylpyridine and ethylene glycol dimethacrylate, P4VPE, with different porosity parameters were tested for Cu(II) sorption from aqueous solutions. Six kinetic models, chemical reaction- and diffusion-based (pseudo-first order (PFO), pseudo-second order (PSO), Elovich, intraparticle diffusion (IPD), Bangham and Boyd model) were used to analyze Cu(II) uptake kinetics in order to define the rate-controlling mechanisms. The nature of interactions between Cu(II) ions and pyridine groups of porous P4VPE was further elucidated by XPS.

EXPERIMENTAL

P4VPE synthesis

4-VP, EGDMA, azo-*α*,*α*'-bisisobutyronitrile (AIBN), *n*-heptane, 2-hydroxyethyl cellulose, gelatin and NaCl were purchased from Sigma-Aldrich. All reagents and solvents were used as supplied, except AIBN which was recrystallized from methanol before use.

Three samples of macroporous crosslinked P4VPE were prepared by a radical suspension copolymerization in a 0.5 dm^3 three-necked round bottom flask [13]. The monomer phase (80.9 g) containing monomer mixture (24.2 g of 4-VP and 10.3 g of EGDMA), AIBN as initiator (0.8 g) and inert component (8.1, 24.3 and 40.5 g of *n*-heptane for samples 1–3, respectively) was suspended in the aqueous phase consisting of 237.6 g of water, 0.46 g of gelatin, 0.46 g of 2-hydroxyethyl cellulose and 4.6 g of NaCl. The copolymerization was carried out at 343 K for 8 h with a stirring rate of 200 rpm. After completion of the reaction, the copolymer particles were washed with water and ethanol, kept in ethanol for 12 h and dried in vacuum at 313 K. Synthesized samples were purified by extraction in a Soxhlet apparatus with ethanol. The copolymer particles were dried in vacuum at 343 K and sieved. For further investigations, the fraction with particle size of 150–500 μm was used.

Sample analysis

The pore size distributions of the samples were determined by mercury intrusion porosimetry (high pressure Carlo Erba porosimeter 2000), operating in the interval of 0.1–200 MPa. Sample preparation was performed at room temperature and pressure of 0.5 kPa. Samples were outgassed at 323 K and 1 mPa for 6 h.

The copolymer samples were analyzed for their carbon, hydrogen and nitrogen content using the Vario EL III device (GmbH Hanau Instruments, Germany). Elemental composition was calculated from multiple determinations of elemental analysis within ±0.2% agreement.

The Cu(II) concentrations were determined by flame atomic absorption spectrometry (FAAS, SpektrAA Varian Instruments). Standard statistical methods were used to determine the mean values and standard deviations for each set of data.

X-ray photoelectron spectroscopy (XPS) was performed with a Surface Science Instruments SSX-100 photoelectron spectrometer with a monochromatic Al Kα X-ray source ($h\nu$ = 1486.6 eV; 1 eV = 1.6022×10^{-19} J). Measurements were carried out at the photoelectron take-off angle of 35° with respect to the sample surface. The resolution of the survey scans was set to 4, and the acquisition of C 1s signal was done at the constant pass energy of 50 eV. All spectra were the averaged results of four measurements. Data analysis was performed with the software package Winspec 2.09. To compensate for the surface charging effect, all the binding energies were referred to the neutral C 1s peak of 284.6 eV. The elemental compositions were calculated with the following relative sensitivity factors: O 1s: 2.49; N 1s: 1.68; C 1s: 1; Si 2s: 1.03; Si 2p: 0.90.

Batch metal-uptake experiments

The sorption of Cu(II) ions from $CuCl_2$ aqueous solutions (initial concentration of 0.05 M) was investigated in batch experiments under non-competitive conditions, at 298 K. P4VPE (2.0 g) was soaked in 5 cm^3 of buffer solution (NaOAc/HOAc, pH 5.5) for 1h. After that, the copolymer was contacted with 72.5 cm^3 of $CuCl_2$ solution (0.05 M) and 72.5 cm^3 of buffer solution. At the appropriate time intervals, the samples were filtered, washed subsequently with water and ethanol, and dried. The remaining solutions were kept for Cu(II) analysis. The reproducibility of the sorption experiments results was verified in triplicate. Standard statistical methods were used to determine the mean values and standard deviations for each set of data and relative standard deviations did not exceed 5.0%. The amount of Cu(II) ions sorbed onto unit mass of macroporous copolymer beads was calculated by using the following expression:

$$Q_t = \frac{(C_i - C_t)V}{m} \quad (1)$$

RESULTS AND DISCUSSION

Samples characterization

Porosity, such an essential characteristic of macroporous copolymers, can be controlled by the type and the amount of the inert component (porogen) and the type and the amount of crosslinking monomer in the reaction mixture [14]. The generally accepted opinion among the leading experts in the field of polymer science is that the difference in the solubility parameters of polymer and inert component, *i.e.*, $|\delta_P - \delta_S|$, can be used as an indication of the inert component impact on the porous structure of copolymers [15]. The solubility parameter, δ_P, for P4VPE (calculated according to the Van Krevelen equation) is 23.6 $(J\ cm^{-3})^{1/2}$ [16]. The literature value of solubility parameter, δ_S, for *n*-heptane is 15.1 $(J\ cm^{-3})^{1/2}$ [17]. Thus, based on the difference in the solubility parameters, *n*-heptane is frequently used as the inert component, *i.e.*, porogen for the synthesis of vinylpyridine macroporous copolymers (as non-solvent) [18–20]. Additionally, the literature data confirm that the pore volume of P4VPD can be increased by adding a non-solvent component in the inert component and/or by increasing the inert component content [21].

The values of porosity parameters (V_s and $d_{V/2}$) of P4VPE were calculated from the cumulative pore volume distribution curves while specific surface was calculated on the basis of the cylindrical pore model as described in literature [22,23]. The relevant P4VPE porosity parameters were previously published and collected in Table 1 [13].

Table 1. Porosity parameters of the synthesized P4VPE samples [13]

Sample	V_S / $cm^3\ g^{-1}$	S_{Hg} / $m^2\ g^{-1}$	$d_{V/2}$ / nm
1	0.20	4.2	830
2	0.74	7.3	1800
3	1.15	8.8	2400

The pyridine content of P4VPE samples calculated from the elemental analysis of nitrogen for samples 1–3 was 5.36, 5.24 and 5.19 mmol g^{-1}, respectively. The theoretical pyridine content of P4VPE samples calculated on the basis of the feed composition, *i.e.*, 4-VP content in the monomer mixture, was 5.45 mmol g^{-1}. The pyridine content calculated from the elemental analysis data is somewhat lower than the theoretical. Although the elemental analysis data for the samples is in fair agreement with the theoretical values, the minor discrepancies can be ascribed to the loss of 4-vinylpyridine due to its solubility in the aqueous phase [24].

Sorption kinetics

From the perspective of potential applications, one of the key properties of the chelating polymers is the rate at which metal sorption attains equilibrium. Rapid sorption of metal ions is advantageous, providing a short residence time required for the completion of the actual process. The previously published results [13] demonstrated the increase of Cu(II) amount sorbed by P4VPE with time, reaching almost 90% of the maximum capacity already after 30 min. The excellent achieved sorption half-time values were comparable with the literature data (3, 5 and 6 min for samples 1–3, respectively). Sugii *et al*. found the $t_{1/2}$ values for Cu(II) and Ni(II) sorption on P4VPD to be 3 and 5 min, respectively [11]. Also, they found higher Cu(II) sorption rates for P4VPE than for P4VPD in the acetate buffer [9]. The $t_{1/2}$ values for Hg(II) sorption on P4VPD quaternized with 2-chloroacetamide were 4 and 14 min from diluted mercury acetate and mercury chloride solutions, respectively [3].

The amount of Cu(II) ions sorbed at equilibrium for sample 3 (Q_{eq} = 1.40 mmol g^{-1}, 89 mg g^{-1}), *i.e.*, the sample with the highest values of pore diameter and specific pore volume was 17.5 times higher than for sample 1 (Q_{eq} = 0.08 mmol g^{-1}, 5.1 mg g^{-1}) and 2 times higher than for sample 2 (Q_{eq} = 0.69 mmol g^{-1}, 44 mg g^{-1}). As the pyridine content in all P4VPE samples is roughly the same, it can be deduced that the porosity parameters of the copolymer samples used in the sorption experiments had the predominant influence on the Cu(II) uptake behavior. The pH value of 5.5 was selected as the optimum, being as close to neutral as possible, but at the same time taking into consideration that at pH values higher than 6 significant hydrolysis of Cu(II) occurs at high concentrations which are the order of magnitude higher than the ones used in this study [25].

Kinetic modeling

The migration rates of metal ions from the bulk solution to the sorbent surface and the accumulation on this surface govern the kinetics of sorption process and thus its efficiency [2]. The analysis of kinetics offers an insight into the possible mechanisms of sorption and reaction pathways. Sorption mechanisms are dependent on sorbate–sorbent interactions and system conditions, making it impossible to classify sorption mechanisms by solute type [26]. A logical classification based on kinetic models was introduced and generally accepted.

Previously published studies indicate that there are four consecutive phases in the sorption of sorbate by a porous sorbent: bulk diffusion, film or boundary layer

diffusion, intraparticle diffusion and finally solute sorption by complexation or physicochemical sorption or ion exchange [26,27]. The overall sorption rate may be principally controlled by any of these steps or a combined effect of a few steps is also probable. The most extensively used kinetic models are those that presume that the final step constitutes the major contribution to the process kinetics [28,29]. This step is referred to as the "surface reaction", not necessarily meaning that the actual chemical reaction occurs on the sorbent surface involving the formation of chemical bonds. These kinetic models are known as surface reaction-based models and they do not take into consideration the possible influence of diffusion in sorption processes. However, if diffusion driven kinetics are presumed, in diffusion-based modeling the typical assumption is that bulk diffusion and solute sorption onto the surface of the sorbent are instantaneous and, therefore, not rate determining. Consequently, the rate-controlling parameter may be distributed between film diffusion and intraparticle diffusion. With the intention of analyzing the controlling mechanism of Cu(II) sorption process by P4VPE, several equations (PFO, PSO, Elovich, IPD, Bangham and Boyd models) were tested against the experimental data.

Surface reaction-based kinetic modeling

A variety of kinetic models have based their description of the reaction order of sorption systems on solution concentration. Alternatively, reaction orders based on the capacity of the sorbent have also been successfully introduced [30]. In all probability, the earliest known and one of the most extensively used kinetic equations so far for the sorption of a solute from a liquid solution is the Lagergren's equation or the PFO equation [31]:

$$\log\left(Q_{\text{eq}} - Q_t\right) = \log Q_{\text{eq}} - \frac{k_1 t}{2.303} \tag{2}$$

A plot of $\log\left(Q_{\text{eq}} - Q_t\right)$ *vs. t* should give a straight line to confirm the applicability of this kinetic model. If the process is strictly first-order, $\log Q_{\text{eq}}$ should be equal to the intercept of the plot $\log\left(Q_{\text{eq}} - Q_t\right)$ *vs. t*.

The PSO rate expression is employed to describe chemisorption involving valence forces through either sharing or exchange of electrons between the sorbent and sorbate as covalent forces, and ion exchange [32]. The PSO equation is applied in the given form [30]:

$$\frac{t}{Q_t} = \frac{1}{k_2 Q_{\text{eq}}^2} + \frac{1}{Q_{\text{eq}}} t \tag{3}$$

A plot of t/Q_t *vs. t* should give a linear relationship for the second-order kinetics. Additionally, the initial sorption rate can be determined using the equation [30]:

$$h = k_2 Q_{\text{eq}}^2 \tag{4}$$

The extensively used PSO equation, sometimes denoted as Ho's, has the following advantages according to its author: It does not have the problem of assigning the effective sorption capacity, and the PSO rate constant and the initial sorption rate all can be calculated from the equation without having prior knowledge of any of the parameters [30]. An additional advantage of the PSO equation for estimating the Q_{eq} values is its reduced sensitivity to the influence of random experimental errors [2]. This equation deserves particular attention as it predicts the behavior over the whole range of studies and is in agreement with chemisorption being the rate controlling step [32]. The relevant parameters calculated from the values of the intercepts and slopes of the corresponding plots for the PFO and the PSO equations are given in Table 2. Plots $\log\left(Q_{\text{eq}} - Q_t\right)$ vs. *t* (PFO) and t/Q_t vs. *t* (PSO) for Cu(II) sorption by P4VPE are shown in Figure 1.

Table 2. Kinetic parameters for Cu(II) uptake using P4VPE samples as sorbent

Parameter	Sorbent		
	1	2	3
Q_{eq} / mmol g^{-1}	0.08	0.69	1.40
Pseudo-first order			
k_1 / min^{-1}	0.049	0.065	0.064
$Q_{\text{eq}}^{\text{calc}}$ / mmol g^{-1}	0.04	0.45	0.89
R^2	0.864	0.946	0.870
Pseudo-second order			
k_2 / g mmol^{-1} min^{-1}	3.97	0.31	0.14
h / mmol g^{-1} min^{-1}	0.03	0.16	0.31
$Q_{\text{eq}}^{\text{calc}}$ / mmol g^{-1}	0.082	0.73	1.48
R	0.999	0.999	0.999
Elovich			
a_{e} / mmol g^{-1} min^{-1}	0.31	0.60	0.96
b_{e} / g mmol^{-1}	95.2	8.16	3.82
R^2	0.962	0.952	0.944
Intraparticle			
k_{id} / mmol g^{-1} min$^{-0.5}$	0.003	0.047	0.13
C_{id} / mmol g^{-1}	0.05	0.39	0.62
R^2	0.987	0.985	0.995
Bangham			
$k_b \times 10^3$ / g^{-1}	0.07	0.43	0.79
α	0.219	0.356	0.477
R^2	0.784	0.804	0.849

The theoretical Q_{eq} values estimated from the first-order kinetic model were not in compliance with the experimental Q_{eq}, and the observed coefficients of determination were rather low. Accordingly, the PFO model is not valid for Cu(II) sorption on P4VPE. On the

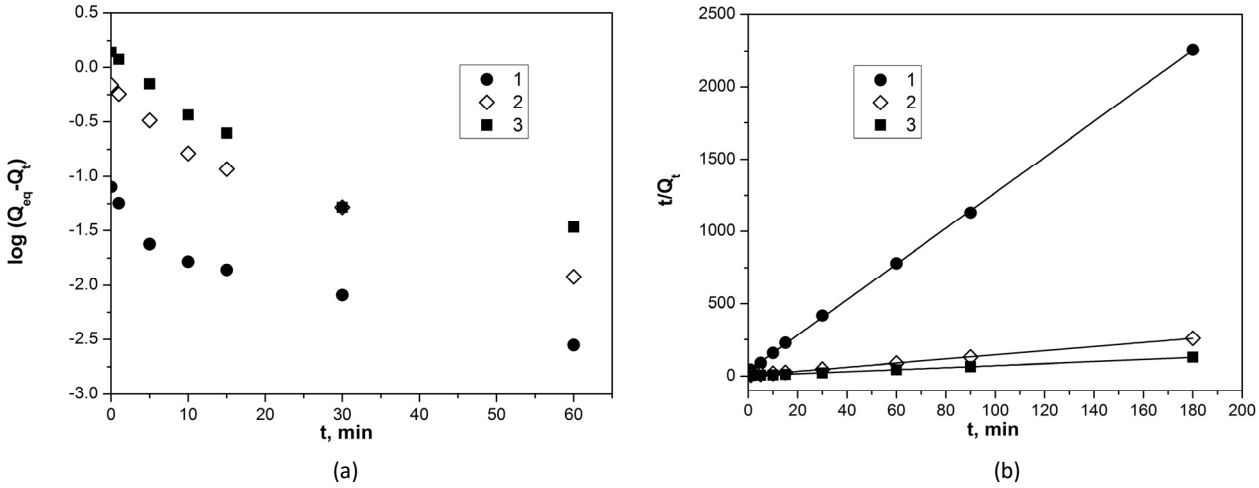

Figure 1. Pseudo-first (a) and pseudo-second order kinetics (b) of Cu(II) uptake by P4VPE samples (sample 1 – black circles, sample 2 – white rhombs, sample 3 – black squares).

other hand, the theoretical Q_{eq} values calculated from the PSO model were found to be in close agreement with the experimental Q_{eq} values with coefficients of determination higher than 0.99. Such R^2 values verify that the sorption data are well represented by PSO kinetics for the whole sorption period and, in consequence, maintain the premises of the model [30].

The initial sorption rate is the highest for the sample with the highest specific pore volume and pore diameter (sample 3), reflecting the greatest availability of sorption centers in this sample and thus the most pronounced affinity of sample 3 for Cu(II) ions. The superior fit of the PSO rate expression to the experimental data indicates that the sorption process is surface reaction-controlled through chemisorption by sharing or exchange of electrons between P4VPE and Cu(II) as covalent forces and/or through ion exchange [30]. In the past decade, the PSO kinetic model has been widely applied to the pollutants sorption from aqueous solutions [30].

The Elovich equation, also successfully employed to describe second-order kinetics is based on the supposition that the actual sorbent surface is energetically heterogeneous and that neither desorption nor interactions between the sorbed species could considerably influence the sorption kinetics at low surface coverage [33]. This equation does not propose any definite mechanism for sorbate-sorbent reaction, but it has been broadly used in sorption kinetics to describe chemisorption through mechanisms which are chemical reactions by nature [34]. The complexity of the original Elovich equation encouraged the habitual use of its simplified linear form [33]:

$$Q_t = \frac{\ln a_e b_e}{b_e} + \frac{1}{b_e}\ln t \qquad (5)$$

The Elovich coefficients a_e and b_e can be calculated from the plots of Q_t *vs*. ln *t* (Figure 2). The relevant kinetic parameters for surface reaction-based kinetic models, as well as coefficients of determination were listed in Table 2.

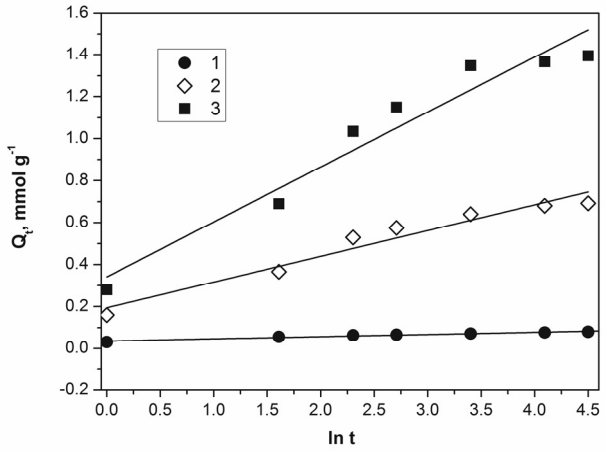

Figure 2. Elovich plots for Cu(II) sorption on PVPE samples (sample 1 – black circles, sample 2 – white rhombs, sample 3 – black squares).

The non-physical behaviour of Eq. (5) for longer sorption times is easily noticeable, *i.e*., $q(t\rightarrow\infty) = \infty$ [28]. Theoretical interpretations of this equation suggest that the underlying reason for such behavior is that the rate of simultaneously occurring desorption is neglected. Consequently, the applicability of the Elovich equation is in practice restricted to the initial times of sorption process, when the system is relatively far from equilibrium [28]. Yet, recent studies demonstrate very similar behavior of the Elovich and the PSO equations under the assumption that the system is not close to equilibrium [28]. Rudzinski and Plazinski have quantitatively proved that in spite of their different mathe-

matical form, both the PSO and the Elovich equations display basically identical behaviour when taking into account the values of fractional surface coverages lower than about 0.7 [29].

Diffusion-based kinetic modeling

Generally, metal sorption by porous sorbents is a multi-step process involving transport of the solute molecules from the aqueous phase to the surface of the solid particulates followed by diffusion into the interior of the pores [26,27]. Thus, diffusional mass transport models, such as film diffusion and intra-particle diffusion, warrant further consideration. Their role is very significant especially in processes where ion exchange and ionic bonding are not as dominant as in chemisorption processes [32].

Since the PFO, the PSO and Elovich kinetic models cannot identify this influence of diffusion on sorption, the Weber and Morris equation was used for calculation of the rate constants of the IPD model [35]. This model presumes that film or boundary layer diffusion is negligible, and that IPD is the only rate-controlling step. The rate of IPD can be calculated according to the equation [36]:

$$Q_t = C_{id} + k_{id} t^{0.5} \quad (6)$$

where C_{id} is the intercept which is proportional to the boundary layer thickness [37]. The values of C_{id} and k_{id} are tabulated in Table 2. The k_{id} value was estimated from the slope of the linear portion of the plot Q_t *vs*. $t^{0.5}$ displayed in Figure 3. If the Q_t *vs*. $t^{0.5}$ plot is linear over the whole time range and if the line passes through the origin, IPD is the only rate-controlling step [38]. If not, it is indicative of involvement of some other mechanisms.

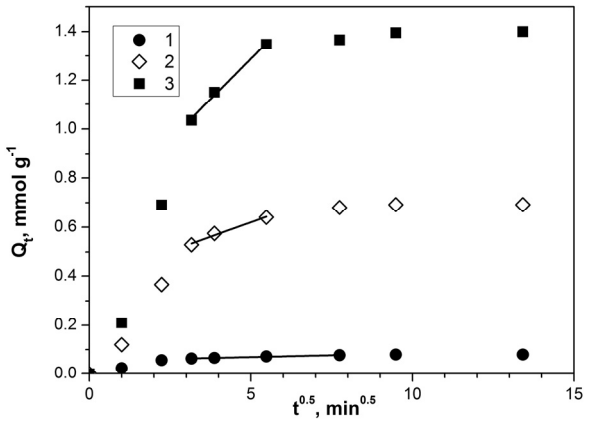

Figure 3. Plots based on intraparticle diffusion model for Cu(II) uptake using P4VPE as sorbent (sample 1 – black circles, sample 2 – white rhombs, sample 3 – black squares).

The plots Q_t *vs*. $t^{1/2}$ presented in Figure 3 for Cu(II) sorption on P4VPE did not pass through the origin suggesting that even though the sorption process included IPD, it was not the only rate-controlling step [38]. The positive value of intercept is indicative of some degree of boundary layer control. Its contribution increases with the increase of k_{id}, *i.e.*, as the surface area and pore diameter become larger. The multilinear shape of Q_t *vs*. $t^{1/2}$ relationships indicates that more than one process governs Cu(II) sorption on P4VPE, too. The first sharper portion (Figure 3) can be regarded as external surface sorption or faster sorption stage, succeeded by gradual sorption where IPD is rate controlling. After that, in the final equilibrium stage IPD slows down due to the low sorbate concentration in solution. Kumar et al. observed the similar behavior for Cr(III) removal by using an amine-based polymer, aniline-formaldehyde condensate (AFC) coated on silica gel [39]. When all other conditions are the same (size of sorbate molecule, sorbate concentration and its affinity towards the sorbent, the diffusion coefficient of the sorbate in the bulk, the degree of mixing), the rate of uptake is limited by the sorbent pore size distribution [38]. In this case, it is apparent from Table 2 that the increase in specific pore volume and pore diameter is crucial for the observed trend in the k_{id} values. IPD is facilitated by the presence of macroporosity.

It is also noticeable that the dependence of the amount of Cu sorbed on the square-root of time has a concave character for all three samples (Figure 3). The model analysis by Plazinski *et al*. has demonstrated that such curve shape may be attributable to a combined effect of the rate of surface reaction and that of the solute transport from the bulk to the surface [28], in support of the conclusions arrived at in the case of this sorbate-sorbent system examined in this paper.

Kinetic data were further analyzed using Bangham's equation in order to confirm that pore diffusion is one of the rate-controlling steps in this sorption system. This equation is commonly expressed as [40]:

$$\log\log\left[\frac{C_i}{C_i - C_s Q_t}\right] = \log\left[\frac{k_b C_s}{2.303V}\right] + \alpha \log t \quad (7)$$

k_b and α are calculated from the intercept and the slope of the straight line plots of log log $[C_i/(C_i - C_s Q_t)]$ *vs*. log t. If this expression is an adequate illustration of experimental data, than the sorption kinetics is limited by pore diffusion [41].

The Bangham plot for P4VPE samples is shown in Figure 4. Bangham´s kinetic parameters were calculated and tabulated in Table 2.

Bangham's plot should be linear if intraparticle diffusion is the only rate controlling step [42]. Non-linearity of the Bangham plots as well as the significant intercept values obtained from the intraparticle diffusion model indicated that both film diffusion as well as pore diffusion were rate-limiting [43]. The correlation coefficients given by the Bangham's equation

verified that the model did not entirely fit the experimental data for Cu(II) sorption on P4VPE.

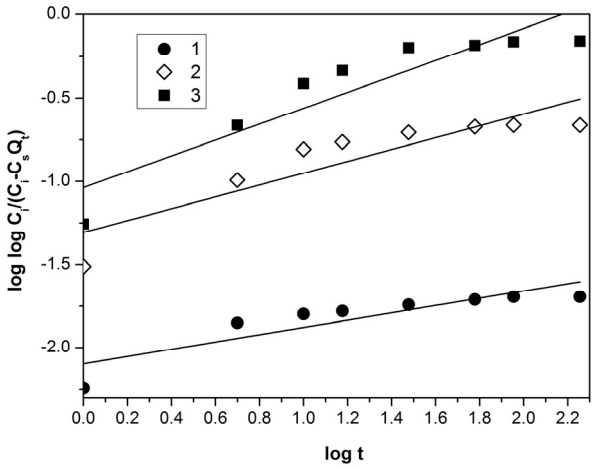

Figure 4. Plot of Bangham's equation for Cu(II) sorption using P4VPE as sorbent (sample 1 – black circles, sample 2 – white rhombs, sample 3 – black squares).

The contribution of boundary layer or film diffusion implied by the non-zero values of the intraparticle plot intercept is often ascertained using the model given by Boyd [36]:

$$F = 1 - \frac{6}{\pi^2}\sum_{n=1}^{\infty}\frac{1}{n^2}\exp\left(-\frac{n^2\pi^2 D_i t}{r^2}\right) \quad (8)$$

$$F = 1 - \frac{6}{\pi^2}\sum_{n=1}^{\infty}\frac{1}{n^2}\exp\left(-n^2 Bt\right) \quad (9)$$

where F is obtained from the expression:

$$F = \frac{Q_t}{Q_{eq}} \quad (10)$$

And

$$B = \frac{D_i\pi^2}{r^2} \quad (11)$$

The approximations for Bt proposed by Reichenberg [44] are as follows:

$$F \text{ values} < 0.85,\ Bt = \left(\pi^{\frac{1}{2}} - \left(\pi - \frac{\pi^2 F}{3}\right)^{\frac{1}{2}}\right) \quad (12)$$

$$F \text{ values} > 0.85,\ Bt = -0.4997 - \ln(1-F) \quad (13)$$

Thus, the value of Bt can be computed for each value of F, and then plotted against time. The linearity of these so-called Boyd plots (Figure 5) was examined to distinguish between sorption controlled by film diffusion and particle diffusion [24]. If the plot is in the form of straight line passing through the origin, this indicates that sorption processes are governed by particle-diffusion mechanisms. If not, they are controlled by film diffusion [45]. From Figure 5, it was observed that the plots were neither linear nor passed through the origin indicating the strong influence of film diffusion during the sorption of Cu(II) on P4VPE, as well.

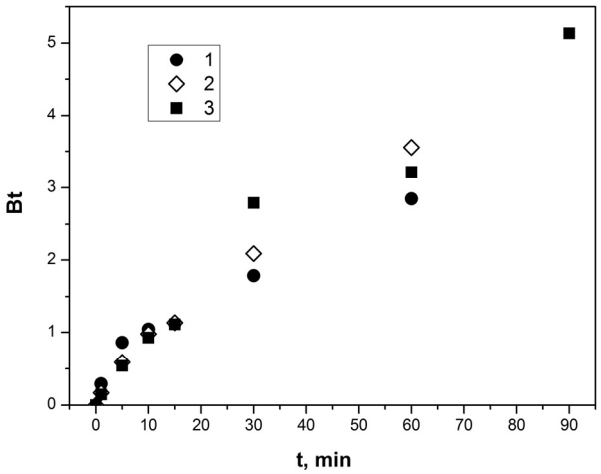

Figure 5. Plots based on Boyd's model for Cu(II) sorption using P4VPE as sorbent (sample 1 – black circles, sample 2 – white rhombs, sample 3 – black squares).

The strong external resistance only during the initial stages of sorption (0–10 min) as seen in Figures 3 and 5 may be mainly due to the absence of mixing and high affinity of the sorbate for the sorbent [46]. Thus, the intraparticle diffusion limits the overall rate of sorption since the investigated systems have high concentration of sorbate and relatively large sorbent particle size of as well as high porosity.

XPS analysis

Positively charged Cu(II) cations form coordination complexes with the nitrogen atom of the pyridine group due to the strong affinity of pyridyl group to metals and its ability to undergo hydrogen bonding, as was established in some previously published studies of P4VPD [12].

XPS measurements were carried out for two P4VPE samples loaded with Cu(II) (Figure 6). Because of the low Q_{eq} value, the results for Sample 1 were omitted from XPS analysis.

Spectral deconvolution of the N 1s XPS spectra of sample 2 (Figure 6a) revealed three distinguishable peaks. The first one at the lowest binding energy of 398.8 eV could be ascribed to the pyridine nitrogen, N(1), [47,48], while the second component at 400.1 eV, N(2), and the third component at 401.6 eV, N(3), were assigned to the pyridine nitrogen interacting with the copper cations and protonated N atoms of P4VPE, res-

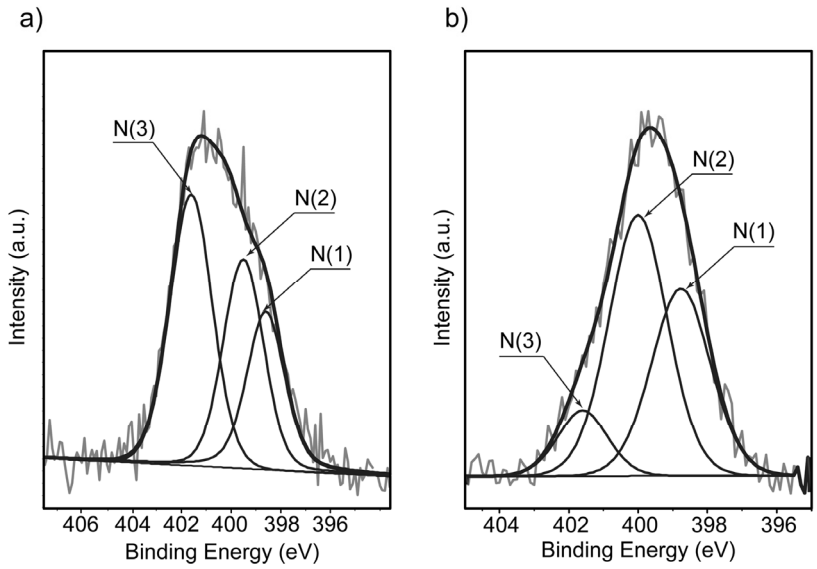

Figure 6. N 1s XPS spectra of P4VPE sample 2 (a) and sample 3 (b) loaded with Cu(II) at pH 5.5 (N(1) = –N, N(2) = –N· · ·Cu^{2+}, N(3) = –NH^{+}).

pectively. Pardey *et al*. reported the N 1s spectrum for poly(4-vinylpyridine), P4VP with a symmetric peak at 399.0 eV and the N 1s spectrum of the fresh and used $CuCl_2$/P4VPD (with 2% of DVB) catalyst with broader and more asymmetric peaks, which could be deconvoluted into two peaks, at 399.0 and 400.3 eV. The peak at 400.3 eV indicated that a fraction of pyridine nitrogen interacts with copper cations [47]. Liu *et al*. observed the peak at 398.6 eV for the pyridine nitrogen in poly(EGDMA-*co*-4VP), PE4VP, and the peak at 400.7 eV for nitrogen atoms in the poly(EGDMA-*co*-4VP) supported-Au nanocolloid [49].

The N 1s peak for Sample 3 was also resolved into three components, *i.e*., the neutral pyridine nitrogen peak at 398.8 eV, N(1), the peak for pyridine nitrogen of 4PVPE interacting with the copper cations at 400.1 eV, N(2) [48] and the peak for the protonated nitrogen atoms at 401.6 eV, N(3). With the copper ions sorbed on the P4VPE, the N 1s XPS spectra in Figure 6a and b show the component of N(2) peak at 400.1 eV, which can be attributed to the nitrogen atoms in the pyridine groups coordinated with copper ions [50]. The nitrogen atoms share a lone pair of electrons with the electron-withdrawing copper ions to form surface complexes. Consequently, the electron density of the nitrogen atoms in the amine groups is reduced and the N 1s binding energy increased (observed at a higher eV value than neutral pyridine N 1s). It can therefore be concluded that the sorption mechanism is based on the formation of metal complexes by the copper ions with the nitrogen atoms in the neutral pyridine groups. In other words, N· · ·Cu^{2+} complexes were formed on the surfaces of P4VPE. The relative peak ratios of N(1), N(2) and N(3) have been calculated from the areas under each peak in the spectra of Figures 6a and 6b and the results are given in Table 3.

Table 3. Positions and content of N 1s peaks of P4VPE samples 2 and 3 loaded with Cu(II)

Data/Sample	Groups and atoms		
	N(1)	N(2)	N(3)
Position, eV	398.8	400.1	401.6
	Content, %		
2	24.5	36.2	39.2
3	35.3	53.3	11.4

Due to the enhanced Cu(II) uptake of sample 3 (Q_{eq} = 1.40 mmol g^{-1}) in comparison to sample 2 (Q_{eq} = = 0.69 mmol g^{-1}), N(3)/N(2) ratio is larger than for sample 3.

CONCLUSION

Three samples of macroporous crosslinked poly(4-vinylpyridine-*co*-ethylene glycol dimethacrylate) (P4VPE) with different porosity parameters were prepared by suspension copolymerization by varying the *n*-heptane amount in the inert component and used as Cu(II) sorbents from aqueous solutions. The samples were characterized by mercury porosimetry, elemental analysis and x-ray photoelectron spectroscopy (XPS). It was established that the porosity parameters of P4VPE have strong influence on the Cu(II) sorption rate. Sorption behavior of Cu(II) on P4VPE and the rate-controlling mechanisms were analyzed using six kinetic models (PFO, PSO, Elovich, IPD, Bangham and Boyd models). XPS study clarified the nature of the formed P4VPE-Cu(II) species.

Acknowledgment

This study was supported by the Ministry of Education, Science and Technological Development, Republic of Serbia (Projects No. TR 37021 and III 43009). The authors thank Prof. Petra Rudolf and the group of surfaces and thin films (Zernike Institute for Advanced Materials, Groningen) for access to the X-ray photoelectron spectrometer. The authors are also grateful to Dana D. Mijović for assisting with the interpretation of XPS data.

List of symbols

a_e	Initial sorption rate from Elovich model (mmol g^{-1} min^{-1})
α	Constant calculated from slope of the Bangham's straight line
B	Time constant (Boyd's model) (min^{-1})
b_e	Parameter related to the extent of surface coverage and activation energy for chemisorption from Elovich model (g $mmol^{-1}$)
C_e	Equilibrium metal ions concentration in solution (mmol dm^{-3})
C_i	Initial metal ions concentration (mmol dm^{-3})
C_{id}	Constant in IPD model (mmol g^{-1})
C_s	Dosage of sorbent (Boyd's model) (g dm^{-3})
C_t	Concentration of Cu(II) ions after sorption time t (mmol dm^{-3})
δ_P	Solubility parameters of polymer and inert component (J $cm^{-3})^{1/2}$
δ_S	Solubility parameters of polymer and inert component (J $cm^{-3})^{1/2}$
D_i	Effective diffusion coefficient of the metal ions in the sorbent phase (cm^2 min^{-1})
$d_{V/2}$	Pore diameter which corresponds to half of pore volume (nm)
F	Fractional attainment of equilibrium at time t (Boyd's model) (min)
h	Initial sorption rate from PSO model (mmol g^{-1} min^{-1})
k_1	PFO rate constant (min^{-1})
k_2	PSO rate constant (g $mmol^{-1}$ min^{-1})
k_b	Constant calculated from the intercept (Bangham's model) (g^{-1})
k_{id}	IPD rate constant (mmol g^{-1} $min^{-0.5}$)
m	Mass of the copolymer beads used for the experiment (g)
n	Integer that defines the infinite series solution (Boyd's model)
PFO	Pseudo-first kinetic model (PFO)
P4VPE	Poly(4-vinylpyridine-*co*-ethylene glycol dimethacrylate)
PSO	Pseudo-second-order (PSO) kinetic model
Q_{eq}	Amount of sorbed metal ions at equilibrium (mmol g^{-1})
Q_e^{cal}	Amount of sorbed metal ions at equilibrium calculated from PSO (mmolg g^{-1})
Q_{max}	Maximum sorption capacity (mmol g^{-1})
Q_t	Amount of metal ions sorbed by the sorbent at time t (mmol g^{-1})
r	Radius of the copolymer bead assumed to be spherical (cm)
R^2	Determination coefficient
S_{Hg}	Specific surface area (m^2 g^{-1})
$t_{1/2}$	Sorption half-time; *i.e*., time required to reach 50% of the total sorption capacity (min)
V	Volume of the aqueous phase (dm^3)
V_s	Specific pore volume (cm^3 g^{-1})

REFERENCES

[1] H.F. Mark, J.I. Kroschwitz, in: Encyclopedia of Polymer Science and Engineering, Wiley New York, 1989, pp 567–587.

[2] S.S. Gupta, K.G. Bhattacharyya, Kinetics of adsorption of metal ions on inorganic materials: a review, Adv. Colloid. Interface Sci. **162** (2011) 39–58.

[3] H.B. Sonmez, N. Bicak, Quaternization of poly(4-vinyl pyridine) beads with 2-chloroacetamide for selective mercury extraction, React. Funct. Polym. **51** (2002) 55––60.

[4] V. Neagu, S. Mikhalovsky, Removal of hexavalent chromium by new quaternized crosslinked poly(4-vinylpyridines), J. Hazard. Mater. **183** (2010) 533–540.

[5] D. Jermakowicz-Bartkowiak, B.N. Kolarz, Poly(4-vinylpyridine) resins towards perrhenate sorption and desorption, React. Funct. Polym. **71** (2011) 95–103.

[6] M. Chanda, G.L. Rempel, Uranium sorption behavior of a macroporous, quaternized poly(4-vinylpyridine) resin in sulfuric acid medium, React. Funct. Polym. **18** (1992) 141–154.

[7] K.R. Ashley, J.R. Ball, A.B. Pinkerton, K.D. Abney, C. Norman, Sorption behavior of pertechnetate on Reillex™ - HPQ anion exchange resin from nitric acid solution, Solvent Extr. Ion Exch. **12** (1994) 239–259.

[8] F.S. Marsh, Reillex™ - HPQ: A new, macroporous polyvinylpyridine resin for separating plutonium using nitrate anion exchange, Solvent Extr. Ion Exch. **7** (1989) 889–908.

[9] A. Sugii, N. Ogawa, K. Harada, K. Nishimura, Metal Sorption of Macroreticular Poly(4-vinylpyridine) Resins Cross-Linked with Oligo(ethylene glycol dimethacrylates), Anal. Sci. **4** (1988) 399–402.

[10] G.G. Talanova, L. Zhong, R.A. Bartsch, New chelating polymers for heavy metal ion sorption, J. Appl. Polym. Sci. **74** (1999) 849–856.

[11] A. Sugii, N. Ogawa, Y. Iinuma, H. Yamamura, Selective metal sorption on cross-linked poly(vinylpyridine) resins, Talanta **28** (1981) 551–556.

[12] I.U. Castro, F. Stüber, A. Fabregat, J. Font, A. Fortuny, C. Bengoa, Supported Cu(II) polymer catalysts for aqueous phenol oxidation**,** J. Hazard. Mater. **163** (2009) 809–815.

[13] A. Nastasović, D. Đorđević, D. Jakovljević, T. Novaković, Z. Vuković, S. Jovanović, Heavy Metal Ions Removal with

Macroporous Poly(4-vinylpyridine-ethylene Glycol Dimethacrylate), in: R.K. Bregg (Ed.), Leading Edge Polymer Research, Nova Science publishers, New York 2006, pp. 213–234.

[14] F. Švec, Interaction of Reactive Sizes of Macroporous Copolymers Glycidyl Methacrylate-Ethylene Dimethacrylate, Angew. Makromol. Chem. **144** (1986) 39–49.

[15] O. Okay, Macroporous copolymer networks, Progr. Polym. Sci. **25** (2000) 711–779.

[16] D.W. van Krevelen, Properties of Polymers, Elsevier, New York, 1990.

[17] H. Burell, Solubility Parameter Values, in: J. Brandrup, E.H. Immergut (eds.), Polymer Handbook, John Wiley, New York, 1975, p. IV 337.

[18] L.C. Santa Maria, A.P. Aguiar, M.R.M.P. Aguiar, A.C. Jandrey, P.I.C. Guimaraes, L.G. Nascimento, Microscopic analysis of porosity of 2-vinylpyridine copolymer networks: 1. Influence of diluent, Mater. Lett. **58** (2004) 563–568.

[19] F.M.B. Coutinho, C.T. Lima Luz, The influence of diluents on the formation of porous structure in ion exchanger resins based on 2-vinylpyridine and divinylbenzene, Eur. Polym. J. **29** (1993) 1119–1123.

[20] C.T. Lima Luz, F.M.B. Coutinho, The influence of the diluent system on the porous structure formation of copolymers based on 2-vinylpyridine and divinylbenzene-diluent system: I. *n*-Heptane/diethylphthalate, Eur. Polym. J. **36** (2000) 547–553.

[21] M.A. Malik, E. Ur-Rehman, R. Naheed, N.M. Alam, Pore volume determination by density of porous copolymer beads in dry state, React. Funct. Polym. **50** (2002) 125–130.

[22] S. Jovanović, A. Nastasović, N. Jovanović, K. Jeremić, Z. Savić, The influence of inert component composition on the porous structure of glycidyl-methacrylate /ethylene glycol dimetacrylate copolymers, Angew. Makromol. Chem. **219** (1994) 161–168.

[23] P.A. Webb, C. Orr, Analytical Methods in Fine Particle Technology, Micromeritics Instrument Corporation, Norcross, GA, 1997, p. 185.

[24] N. Hird, M.G.J.T. Morrison, D.C. Sherrington, J.C. Trillow, Tailoring of 4-vinylpyridine-based resins for hydrolytic degradation and solubilisation, Tetrahedron **55** (1999) 9585–9594.

[25] R. Djeribi, O. Hamdaoui, Sorption of copper(II) from aqueous solutions by cedar sawdust and crushed brick, Desalination **225** (2008) 95–112.

[26] Y.S. Ho, J.C.Y. Ng, G. McKay, Kinetics of pollutant sorption by biosorbents: review, Sep. Purif. Methods **29** (2000) 189–232.

[27] C.Y. Kuo, C.H. Wu, J.Y. Wu, Adsorption of direct dyes from aqueous solutions by carbon nanotubes: Determination of equilibrium, kinetics and thermodynamics parameters, J. Colloid Interface Sci. **327** (2008) 308–315.

[28] W. Plazinski, W. Rudzinski, A. Plazinska, Theoretical models of sorption kinetics including a surface reaction mechanism: a review, Adv. Colloid Interface Sci. **152** (2009) 2–13.

[29] W. Rudzinski, W, Plazinski, On the applicability of the pseudo-second order equation to represent the kinetics of adsorption at solid/solution interfaces: a theoretical analysis based on the statistical rate theory, Adsorption **15** (2009) 181–192.

[30] Y.S. Ho, Review of second-order models for adsorption systems, J. Hazard. Mater. **B136** (2006) 681–689.

[31] S. Lagergren, About the theory of so-called adsorption of soluble substances, K. Sven. Vetenskapsakad. Handl. **24** (1898) 1–39.

[32] Y.S. Ho, G. McKay, A comparison of chemisorption kinetic models applied to pollutant removal on various sorbents, Process Saf. Environ. Prot. (Trans. Ichem. E Part B) **76** (1998) 332–340.

[33] D.L. Sparks, Kinetics of Soil Chemical Processes, Academic Press Inc., New York, 1989.

[34] F.C. Wu, R.L. Tseng, R.S. Juang, Characteristics of Elovich equation used for the analysis of adsorption kinetics in dye chitosan systems, Chem. Eng. J. **150** (2009) 366–373.

[35] W.J. Weber, J.C. Morris, Kinetics of adsorption on carbon from solution, J. Sanit. Eng. Div. AM. Soc. Civ. Eng. **89** (1963) 31–60.

[36] G.E. Boyd, A.W. Adamson, L.S. Myers, The exchange adsorption of ions from aqueous solutions by organic zeolites, II: kinetics, J. Am. Chem. Soc. **69** (1947) 2836–2842.

[37] A.M. Donia, A.A. Atia, W.A. Al-Amrani, A.M. El-Nahas, Effect of structural properties of acid dyes on their adsorption behaviour from aqueous solutions by amine modified silica, J. Hazard. Mater. **161** (2009) 1544–1550.

[38] A.S. Özcan, A Özcan, Adsorption of acid dyes from aqueous solutions onto acid-activated bentonite, J. Colloid Interface Sci. **276** (2004) 39–46.

[39] P.A. Kumar, M. Ray, S. Chakraborty, Adsorption behaviour of trivalent chromium on amine-based polymer aniline formaldehyde condensate, Chem. Eng. J. **149** (2009) 340–347.

[40] A. Bhatnagar, A.K. Jain, A comparative adsorption study with different industrial wastes as adsorbents for the removal of cationic dyes from water, J. Colloid Interface Sci. **281** (2005) 49–55.

[41] E. Tutem, R. Apak, C.F. Unal, Adsorptive removal of chlorophenols from water by bituminous shale, Water. Res. **32** (1998) 2315–2324.

[42] I.D. Mall, V.C. Sivastava, N.K. Agarwal, Removal of Orange-G and methyl violet dyes by adsorption on to bagasse fly ash – kinetic study and equilibrium isotherm analyses, Dyes Pigments **69** (2006) 210–223.

[43] M.A. Malana, R.B. Qureshi, M.N. Ashiq, Adsorption studies of arsenic on nano aluminium doped manganese copper ferrite polymer (MA, VA, AA) composite: Kinetics and mechanism, Chem. Eng. J. **172** (2011) 721–727.

[44] D. Reichenberg, Properties of Ion-Exchange Resins in Relation to their Structure. III. Kinetics of Exchange, J. Am. Chem. Soc. **75** (1953) 589–597.

[45] D. Mohan, K.P. Singh, Single- and multi-component adsorption of cadmium and zinc using activated carbon

derived from bagasse—an agricultural waste, Water. Res. **36** (2002) 2304–2318.

[46] V. Vadivelan, K.V. Kumar, Equilibrium, kinetics, mechanism, and process design for the sorption of methylene blue onto rice husk, J. Colloid Interface Sci. **286** (2005) 90–100.

[47] A.J. Pardey, A.D. Rojas, J.E. Yánez, P. Betancourt, C. Scott, C. Chinea, C. Urbina, D. Moronta, C. Longo, Spectroscopic characterization of coordination complexes based on dichlorocopper(II) and poly(4-vinylpyridine): Application in catalysis, Polyhedron **24** (2005) 511–519.

[48] N. Graf, E. Yegen, T. Gross, A. Lippitz, W. Weigel, S. Krakert, A. Terfort, W.E.S. Unger, XPS and NEXAFS studies of aliphatic and aromatic amine species on functionalized surfaces, Surf. Sci. **603** (2009) 2849–2860.

[49] W. Liu, X. Yang, L. Xie, Size-controlled gold nanocolloids on polymer microsphere-stabilizer *via* interaction between functional groups and gold nanocolloids, J. Colloid Interface Sci. **313** (2007) 494–502.

[50] C. Liu, R. Bai, L. Hong, Diethylenetriamine-grafted poly-(glycidyl methacrylate) adsorbent for effective copper ion adsorption, J. Colloid Interface Sci. **303** (2006) 99––108.

IZVOD

IMOBILIZACIJA Cu(II) POMOĆU JEDNOSTEPENO SINTETISANOG POLI(4-VINILPIRIDIN-*CO*-ETILEN--GLIKOLDIMETAKRILATA): ANALIZA KINETIKE SORPCIJE I XPS KARAKTERIZACIJA PRODUKATA

Danijela D. Maksin[1], Aleksandra B. Nastasović[2], Tatjana N. Maksin[1], Zvjezdana P. Sandić[1,3], Katja Loos[4], Bojana M. Ekmeščić[2], Antonije E. Onjia[1]

[1]*Univerzitet u Beogradu, Institut za nuklearne nauke "Vinča", Beograd, Srbija*
[2]*Univerzitet u Beogradu, IHTM – Centar za hemiju, Beograd, Srbija*
[3]*Univerzitet u Banja Luci, Prirodno–matematički fakultet, Banja Luka, BiH (Republika Srpska)*
[4]*Department of Polymer Chemistry, Zernike Institute for Advances Materials, University of Groningen, Groningen, The Netherlands*

(Naučni rad)

U okviru ovog rada sintetizovan je kopolimer na bazi 4-vinilpiridina i ispitana mogućnost njegovog korišćenja za sorpciju Cu(II). Tri umrežena makroporozna uzorka poli(4-vinilpiridin-co-etilenglikoldimetakrilata) (P4VPE) sa različitim parametrima porozne strukture sintetizovani su suspenzionom kopolimerizacijom. Parametri porozne strukture su podešavani variranjem udela *n*-heptana u inertnoj komponenti. Uzorci su okarakterisani živinom porozimetrijom, elementarnom analizom i rendgenskom fotoelektronskom spektroskopijom (XPS). Zapažene su relativno velike brzine sorpcije Cu(II) jona na uzorcima P4VPE pri nekompetitivnim uslovima, odnosno, vrednost maksimalnog kapaciteta se dostiže za 30 min. Maksimalni kapacitet sorpcije za uzorak sa najvećom vrednošću prečnika pora i specifične zapremine pora (uzorak 3, Q_{eq} = 89 mg g^{-1}) je 17,5 puta veći od kapaciteta za uzorak sa najmanjom vrednošću prečnika pora i specifične zapremine pora (uzorak 1, Q_{eq} = 5,1 mg g^{-1}). Budući da je sadržaj piridinskih grupa skoro isti u svim uzorcima P4VPE, zaključeno je da na brzinu sorpcije Cu(II) jona odlučujući uticaj imaju parametri porozne strukture uzoraka. Kinetika sorpcije je analizirana pomoću šest kinetičkih modela (pseudo-prvog, pseudo-drugog reda, Eločičevog, unutarčestične difuzije, Bangamovog i Bojdovog modela) da bi se odredilo koji model najbolje opisuje sorpciju Cu(II) jona pomoću P4VPE. Priroda interakcija P4VPE–Cu(II) vrsta nastalih sorpcijom razjašnjena je metodom fotoelektronske spektroskopije x-zracima.

Ključne reči: 4-Vinilpiridin • Makroporozni kopolimer • Kinetika sorpcije • XPS